

Topological edge states in the one-dimensional super-lattice Bose-Hubbard model

Fabian Grusdt^{1,2}, Michael Hoening¹, and Michael Fleischhauer¹

¹ Dept. of Physics and Research Center OPTIMAS, Technische Universität Kaiserslautern, D-67663 Kaiserslautern, Germany

² Graduate School Materials Science in Mainz, Technische Universität Kaiserslautern, D-67663 Kaiserslautern, Germany

(Dated: January 31, 2013)

We analyze the ground state of interacting ultra-cold bosonic atoms in a one-dimensional (1D) super-lattice potential with alternating tunneling rates t_1 and t_2 . A topological order parameter is introduced which is quantized in units of π for the Mott insulating (MI) phases. A step in the effective confining potential created e.g. by a second heavy atom species can lead to an interface between two MI regions with filling $n = 1$ and $n = 1/2$. Depending on the ratio t_1/t_2 the $n = 1/2$ MI phase is topologically non-trivial which results in localized, protected many-body edge states. Density-matrix renormalization group (DMRG) simulations show that the edge states manifest themselves either in localized density minima or localized density maxima at the interface, which can easily be detected. Shape and energy of the edge states as well as conditions for their occupation are determined analytically in the strong coupling limit and in general by DMRG simulations.

PACS numbers: 05.30.Fk, 03.75.Hh, 73.21.Cd

Topological phases have become an intensively studied subject in many fields of physics. Key features of condensed-matter systems such as topological insulators [1–3] or superconductors [4] as well as quantum Hall systems [5–8] have been related to the existence of robust edge states at interfaces between phases with different topological character. Currently there is a growing activity in condensed-matter physics aiming at creating and understanding novel topological phases. On the other hand ultra-cold atomic gases have developed into an ideal experimental testing ground for concepts of solid-state and many-body physics [9] and they could become important for studying topological effects [10–13]. One of the simplest models possessing non-trivial topological properties is the Su-Schrieffer-Heeger (SSH) model [14], which can be realized by ultra-cold fermions in a 1D tight-binding super-lattice (SL) potential with alternating hopping amplitudes. Its topological properties on a single-particle level have recently been explored both theoretically [15, 16] and experimentally [13]. Here we show that in the case of bosons, MI phases with filling $n = 1/2$ can be non-trivial topological insulators. In this case, introducing a localized potential step, realized e.g. by the admixture of a second, heavy atomic species, allows to create an interface between gapped MI phases with different topological invariants. We show that at the interface, a localized and robust many-body edge state emerges which manifests itself in density minima or maxima that can easily be observed with techniques developed in recent years [17–19]. The edge state, which is an indicator of the topology of the bulk phases, is shown to survive until the insulating phases melt due to tunneling.

The starting point of the discussion is the 1D SL-Bose-Hubbard model (SL-BHM) in the grand-canonical ensemble described by the Hamiltonian $\hat{K} = \hat{H} - \mu\hat{N}$

$$\begin{aligned} \hat{K} = & - \sum_{j \text{ odd}} \left(t_1 \hat{a}_j^\dagger \hat{a}_{j+1} + \text{h.a.} \right) - \sum_{j \text{ even}} \left(t_2 \hat{a}_j^\dagger \hat{a}_{j+1} + \text{h.a.} \right) \\ & + \frac{U}{2} \sum_j \hat{n}_j (\hat{n}_j - 1) + \sum_j (\epsilon_j - \mu) \hat{n}_j, \end{aligned} \quad (1)$$

where \hat{a}_j and \hat{a}_j^\dagger are the annihilation and creation operators of

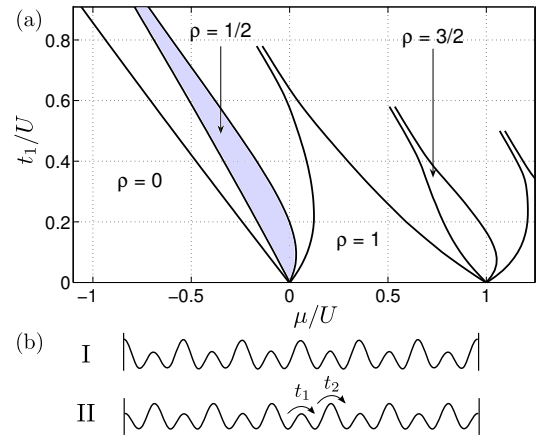


FIG. 1: (Color online) (a) Phase diagram for the SL-BHM with $t_2 = 0.2t_1$ obtained by DMRG. One recognizes the presence of MI phases with integer and half-integer filling. (b) Different dimerizations I and II of SL potential corresponding to Zak phases $\nu^I = 0$ and $\nu^{II} = \pi$.

the bosons at lattice site j , and $\hat{n}_j = \hat{a}_j^\dagger \hat{a}_j$. Particles can tunnel from a lattice site to a neighboring one with alternating hopping amplitudes t_1 and t_2 and there is an on-site interaction U . ϵ_j describes a potential which can also include a slowly varying harmonic confinement, and μ is the chemical potential. Eq. (1) corresponds to the SSH model in the case of fermions (where the interaction term is absent) or in the equivalent case of hard-core bosons ($U \rightarrow \infty$).

A generic ground-state phase diagram of the SL-BHM is shown in Fig.1, which is taken from Ref.[20]. Besides MI phases with integer filling, known from the simple BHM, it shows loophole-type insulating regions with half integer filling for $t_1 > t_2$ [21, 22]. These phases shrink in size when t_1 decreases, and vanish at $t_1 = t_2$, i.e. in the case of simple BHM. They reappear when $t_1 < t_2$ and the point $t_1 = t_2$ marks a topological phase transition.

In the case of non-interacting fermions, the topology of the band structure is determined by its Zak phase [23] (or winding number), $\nu = i \int_0^{2\pi} dk \langle u(k) | \partial_k | u(k) \rangle$, where $|u(k)\rangle$ are

t_1/U	0.74	0.25	0.050	0.010
$ \nu_{1/2}^I/\pi $	$3.1 \cdot 10^{-13}$	$6.1 \cdot 10^{-15}$	$1.0 \cdot 10^{-15}$	$4.4 \cdot 10^{-15}$
$ \nu_{1/2}^{II}/\pi - 1 $	$7.9 \cdot 10^{-15}$	$3.0 \cdot 10^{-15}$	$8.9 \cdot 10^{-16}$	$1.4 \cdot 10^{-15}$
$\nu_{5/12}^I/\pi$	-0.27	0.54	-0.12	0.85
$\nu_{5/12}^{II}/\pi$	-0.042	0.13	-0.46	0.0082

TABLE I: Numerical values of the many-body winding number ν , for a $n = 1/2$ MI of $N = 5$ particles ($\nu_{1/2}^I$, upper block) and for $N = 5$ particles on 12 sites ($\nu_{5/12}^I$, lower block) corresponding to a compressible phase. In the MI case, for both $t_2/t_1 = 2$ (upper lines) and $t_2/t_1 = 1/2$ (lower lines) ν is quantized in units of π within the numerical precision.

the single-particle Bloch functions and k is the lattice quasi-momentum. While for a general 1D band structure this phase may take arbitrary values, it is integer quantized (in units of π) [24] when the sub-lattice symmetry is present. In the case of the SSH model the winding numbers of the upper and lower band are equal but opposite $\nu = 0 (\pm\pi)$ [33] for dimerization I (II), see Fig. 1.

For interacting systems there is no conserved lattice quasi-momentum k and we must construct a many-body generalization of the winding number. Like the Chern number [30] it can be defined via generalized boundary conditions, $\psi(x_j + L) = e^{i\theta/L} \psi(x_j)$ for all particle coordinates $j = 1, \dots, N$ and system size L . They correspond to a magnetic flux θ threading the system. When this flux is adiabatically varied, the many-body wavefunction $|\Psi(\theta)\rangle$ picks up a Berry phase [31]

$$\nu = i \int_0^{2\pi} d\theta \langle \psi(\theta) | \partial_\theta | \psi(\theta) \rangle. \quad (2)$$

This topological order parameter can easily be calculate in the hard-core limit $U \rightarrow \infty$. In this case the $n = 1/2$ MI phase is well described by $|\Psi_{1/2}\rangle = \prod_j \int_0^L dx w_1(x - R_j) \hat{\Psi}^\dagger(x) |0\rangle$, where w_1 denotes the Wannier function of the lower SSH band and the lattice vectors R_j are Wannier centers. A similar expression holds for the $n = 1$ MI phase, where also the higher SSH band is filled. We find that the MIs with integer filling are topologically trivial with $\nu = 0$ and those with half-integer filling can take the values $\nu^I = 0$ for dimerization I and $\nu^{II} = \pi$ for dimerization II.

Most importantly numerical exact diagonalization of small systems shows that the topological invariant stays strictly quantized even for finite U as long as the particle-hole gap remains finite (see table I). Thus we expect that the non-trivial topology of the SSH bands for free fermions carries over to bosons with finite interactions. This is our motivation to study edge states between topologically distinct MI phases in the SL-BHM as indicators for a quantized topological invariant.

An interface can be created in ultra-cold lattice gases as follows: An increase of the potential energy ϵ_j in the Hamiltonian (1) corresponds to a shift in the chemical potential. Thus an increase of ϵ_j for a number of consecutive lattice sites by $\Delta\epsilon$ can lead to an interface between two MI phases with integer (e.g. $n = 1$) and half-integer filling (e.g. $n = 1/2$). This

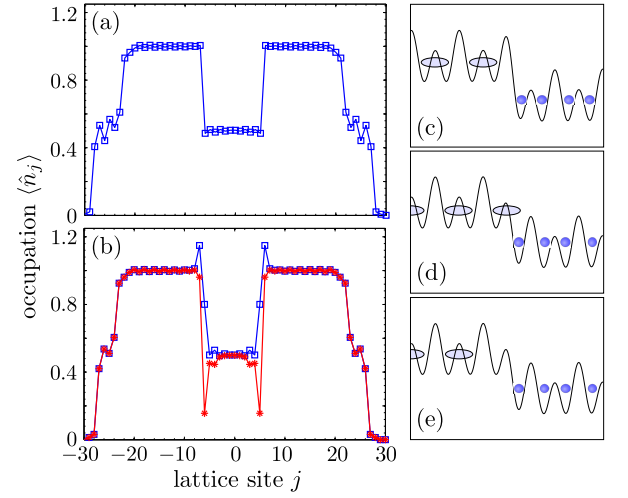


FIG. 2: (Color online) Ground-state density distribution of the SL-BHM with harmonic trap and additional potential step between sites $j = -6$ and $j = 5$ leading to interfaces between $n = 1/2$ (in the center) and $n = 1$ MI regions. $\epsilon_j^{\text{trap}} = \omega(j + 0.5)^2$, with $\omega/U = 0.001$. Results are obtained by DMRG simulations for $\mu/U = 0.55$. (a) topological trivial $n = 1/2$ MI phase with $t_1/U = 0.04$, $t_2/U = 0.2$ and $\Delta\epsilon/U = 0.6$. (b) topological non trivial $n = 1/2$ phase with $t_1/U = 0.2$, $t_2/U = 0.04$ and $\Delta\epsilon/U = 0.6$ (blue squares), 0.7 (red stars). Right panel illustrates interface in topologically trivial case (c) and in nontrivial case with occupied (d) and unoccupied interface (e).

can be realized if μ and $\Delta\epsilon$ are chosen such that

$$\mu_-^1 < \mu < \mu_+^1 \quad (3)$$

$$\mu_-^{1/2} + \Delta\epsilon < \mu < \mu_+^{1/2} + \Delta\epsilon. \quad (4)$$

Here $\mu_{\pm}^{1/2}$ and μ_{\pm}^1 denote the upper (+) and lower (−) boundary of the insulating regions in the phase diagram of Fig.1. As shown e.g. in Ref.[32] for the case of bose-fermi mixtures, an effective potential step can be created by an admixture of a second atomic species, e.g. fermions, with very small hopping rates. Under appropriate conditions (see [32]) a repulsive, local interaction V between the two species results in an effective attraction of the fermions. With a weak harmonic confinement the fermions form a connected cluster at the center of the trap with unity filling and sharp boundaries if the resulting binding energy exceeds their hopping. This results in an increase of the potential energy of the bosons $\Delta\epsilon = V$ which extends over all sites of the fermion cluster. If $\Delta\epsilon$ and μ fulfill (3) and (4), two interfaces between a $n = 1/2$ MI at the center of the trap and surrounding $n = 1$ MI regions are created. Depending on the location of the interfaces relative to the sub-lattices the winding number either stays, $\Delta\nu = \nu_{1/2}^I - \nu_1 = 0$, or jumps, $\Delta\nu = \nu_{1/2}^{II} - \nu_1 = \pi$.

Fig. 2 shows the density distribution in a weak harmonic trap with an additional potential step $\Delta\epsilon$ calculated by density-matrix renormalization group algorithm (DMRG) [25–27]. One clearly recognizes interfaces between a central $n = 1/2$ MI and surrounding $n = 1$ MI regions. Since the number of heavy particles was taken to be even, both inter-

faces are characterized by the same change $|\Delta\nu|$ in the winding number. The upper plot shows the case $\Delta\nu = 0$, the lower one $\Delta\nu = \pi$. In the first case there is a simple step in the density and no additional structure at the edge. The same holds at an interface between any two MI phases with integer fillings irrespective of the dimerization. In the second case, however, one sees pronounced dips or peaks in the average density. We will argue now that these are clear signatures of the edge state which must be present at any interface between topologically distinct bulk phases.

To understand the origin of the topological edge state, we note that in the hard-core limit $U \rightarrow \infty$ our situation corresponds to free fermions and an interface between a half filled SSH band ($n = 1/2$ side) and completely filled SSH band ($n = 1$ side). With an open boundary and for dimerization II (see Fig.1b) a state with energy $E = 0$ appears between the two half bands which are separated by a finite gap for $t_1 \neq t_2$, while for dimerization I there is no such state. If only the lower SSH half-band is filled the mid-gap state leads either to a peak in the density distribution at the boundary if it is occupied by a fermion or to a dip if it is not occupied. On the other hand for complete filling no such structure exists, as is the case for dimerization I. This is the essence of the edge state counting formula [16] which states that at an open boundary of a topologically nontrivial phase with $\nu = \pi$ exactly one localized edge state exists, which can be occupied by a fermion or not. If the open boundary is replaced by an interface between a half filled and a fully filled band, the finite tunneling t_1 leads to a renormalization of the energies of the two mid-gap states, which remain however within the corresponding gaps. In the following we discuss what happens if the interaction U becomes finite which leads to a mixing of single-particle states.

We start by discussing the properties of the edge states in the limit of large interactions $U \gg t_1$ and small hopping $t_2 \ll t_1$. This allows a perturbation expansion in t_2 and $1/U$ ("cell strong coupling perturbative expansion", CSCPE [28, 29]). We note that the same analysis applies for an interface between any $\frac{m+1}{2}$ and $\frac{m}{2}$ MIs, with m being an integer. In this case the low lying bands can be assumed inert and only lead to a renormalized hopping due to Bose enhancement. We discuss the grand-canonical ground state and consider states ψ_1 and ψ_0 with and without an additional particle at the interface, see Figs.2d and e. The critical chemical potentials defining the borders of the MI phases in the bulk in Fig.1 can easily be calculated in CSCPE. We find up to terms of order $\mathcal{O}(t_2^2/U, t_2 t_1^2/U^2)$

$$\begin{aligned}\mu_+^1 &= -2t_2 - t_1 - \sqrt{2t_1 U + 4t_1^2 + U^2} - \frac{t_2^2}{t_1} \\ &\quad + \frac{3U}{2} + \frac{1}{2}\sqrt{16t_1^2 + U^2} - \frac{4t_1 t_2}{U}, \\ \mu_-^1 &= t_2 + t_1 + \frac{1}{2}\left(U - \sqrt{16t_1^2 + U^2}\right) + \frac{4t_1 t_2}{U} + \frac{t_2^2}{2t_1}, \\ \mu_+^{1/2} &= -t_2 + t_1 + \frac{1}{2}\left(U - \sqrt{16t_1^2 + U^2}\right) - \frac{4t_1 t_2}{U}, \\ \mu_-^{1/2} &= t_2 - t_1.\end{aligned}$$

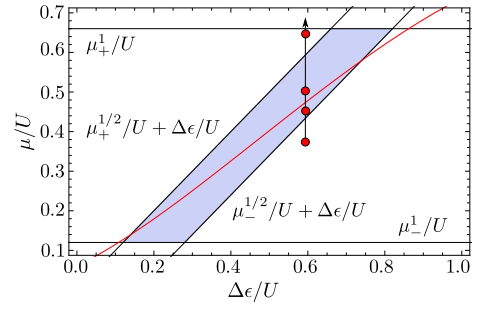


FIG. 3: (Color online) The red line, $\mu_c = E_\epsilon^{(1)} - E_\epsilon^{(0)}$, separates parameter regions with an occupied edge state (upper part) or unoccupied edge state (lower part). When it is within the shaded region, it also indicates stability of the edge states towards hybridization with the bulk. Parameters are $t_1/U = 0.2$ and $t_1/t_2 = 5$.

To understand whether the edge state is actually bound to the interface or hybridizes with the bulk, we perform a stability analysis. We therefore investigate under what conditions the many-body state ψ_1 lies within the gap to collective excitations on the ground state ψ_0 . In this case *both* many-body states $\psi_{0,1}$ constitute a localized particle or hole at the edge and we call the edge state stable. By tuning μ both states can be made the grand-canonical ground state. Hybridization can occur if a particle or a hole excitation is created in the bulk of either of the two MIs. Reducing (increasing) the number of particles at the MI interface by one and simultaneously creating a particle (hole) in the bulk costs a finite energy if

$$\mu_-^1 < E_\epsilon^{(1)} - E_\epsilon^{(0)} < \mu_+^1 \quad (5)$$

$$\mu_-^{1/2} + \Delta\epsilon < E_\epsilon^{(1)} - E_\epsilon^{(0)} < \mu_+^{1/2} + \Delta\epsilon. \quad (6)$$

Here $E_\epsilon^{(0,1)}$ denote the energies of $\psi_{0,1}$ and CSCPE yields

$$\begin{aligned}E_\epsilon^{(1)} - E_\epsilon^{(0)} &= \Delta\epsilon \left(\frac{1}{2} - 2\frac{t_1^2}{U^2} \right) - \frac{t_2^2}{2t_1} - \frac{t_2^2}{2\Delta\epsilon} \\ &\quad - \frac{(4t_1^2 + 5t_2^2)}{U} + \frac{1}{2}\sqrt{\Delta\epsilon^2 + 4t_1^2} + \mathcal{O}(t_2^2/U, 1/U^3)\end{aligned} \quad (7)$$

From Fig.3 one can read off the potential heights $\Delta\epsilon$ for which non of the states $\psi_{0,1}$ hybridizes with the bulk: The red line has to be within the shaded area. Moreover, ψ_0 (ψ_1) is the grand-canonical ground state for a chemical potential $\mu < \mu_c$ ($\mu > \mu_c$) with $\mu_c = E_\epsilon^{(1)} - E_\epsilon^{(0)}$. For $\mu > \mu_c$, i.e. above the red line in Fig.3, the edge state is occupied, while below it is not. The first case (ψ_0) can be detected by measurement of a density less than $1/2$ on the $n = 1/2$ MI side of the interface, the second (ψ_1) by measurement of a density larger than 1 on the $n = 1$ MI side.

To verify these results we performed numerical simulations for a step potential $\epsilon_j/U = \Delta\epsilon\Theta(j - j_{\text{step}} + 0.5)$, where Θ is the Heaviside step function. In Fig.4a we show DMRG results for the density as a function of μ . For $\mu/U = 0.45$ the system is inside the stability region of Fig.3 above the red line. One clearly recognizes a well localized dip in the density. $\mu/U = 0.50$ corresponds to an occupied edge inside

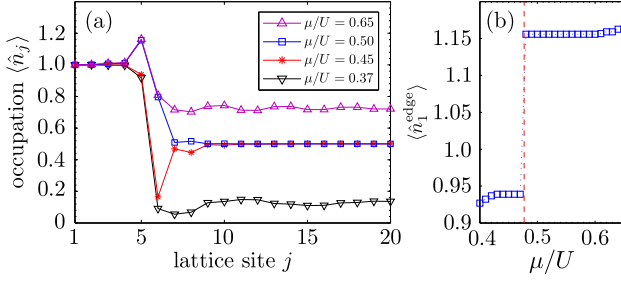


FIG. 4: (Color online) (a) Density distribution at potential step $\Delta\epsilon/U = 0.6$ at $j_{\text{step}} = 6$ for $t_1/U = 0.2$, $t_1/t_2 = 5$ and increasing chemical potential μ/U . (b) Density $\langle\hat{n}_1^{\text{edge}}\rangle$ at the edge of the $n = 1$ MI region as function of μ/U showing the occupation at the edge if $\mu > \mu_c = 0.47$ (dashed red line).

the stability region. Here a clearly pronounced density peak appears. When μ is chosen such that the system is outside the region of the $n = 1/2$ Mott insulator ($\mu/U = 0.37$ and $\mu/U = 0.65$) the density dip on the $n = 1/2$ side starts to vanish while the peak on the $n = 1$ MI side remains. Fig.4b shows the density $\langle\hat{n}_1^{\text{edge}}\rangle$ at the edge of the $n = 1$ MI side as function of μ/U . As soon as μ exceeds μ_c (red dashed line), there is a clear jump indicating the transition from occupied to unoccupied edge.

A particular feature of the edge state in the SL-BHM, not present in the hard-core limit, is the peak of the local density on the border of the $n = 1$ MI region above unity. Within CSCPE we can calculate this density, which yields in zeroth order of t_2

$$\langle\hat{n}_1^{\text{edge}}\rangle = 1 + \frac{4\Delta\epsilon t_1^2}{U^3} + \frac{6\Delta\epsilon^2 t_1^2}{U^4} + \mathcal{O}(1/U^5). \quad (8)$$

Fig.5a shows a comparison of $\langle\hat{n}_1^{\text{edge}}\rangle$ obtained by DMRG with eq.(8) (green, dashed line). Also shown is the CSCPE result in second order in t_2 . The corresponding analytic expression can easily be obtained but is too involved to be given here. One recognizes very good agreement even for rather large tunneling rates just before the $n = 1$ MI starts to melt. For $t_1/U \rightarrow 0$, $\langle\hat{n}_1^{\text{edge}}\rangle$ approaches the hard-core value, while finite tunneling leads into $\langle\hat{n}_1^{\text{edge}}\rangle > 1$. Beyond some optimum value of t_1/U the edge state starts to delocalize as the particle-hole gap of the insulator becomes smaller and $\langle\hat{n}_1^{\text{edge}}\rangle$ decreases. Finally Fig.5b shows density distributions for the occupied and unoccupied edge for $t_1/U = 0.5$, i.e. close to the melting point of the $n = 1$ MI phase. One clearly sees that the edge state is still stable and localized.

In summary we have discussed topological properties of the 1D superlattice Bose-Hubbard model with alternating hopping rates t_1 and t_2 . In the limit of infinite interaction U this model corresponds to the SSH model for free fermions, which is known to possess topologically non-trivial insulating phases for $t_1 \neq t_2$. We introduced a many-body generalization of the Zak phase as topological order parameter. Based on small system exact diagonalization we argued that also for the bosonic model with finite interactions this order parameter is strictly quantized for the Mott insulating phases. To ver-

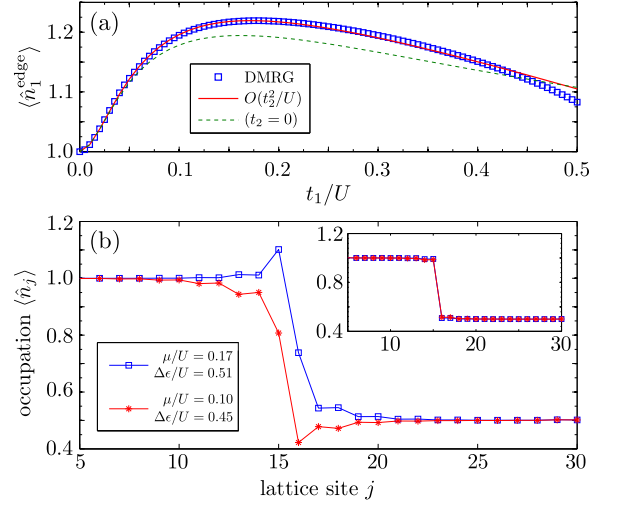


FIG. 5: (Color online) (a) Density $\langle\hat{n}_1^{\text{edge}}\rangle$ at the edge of the $n = 1$ MI region as function of t_1/U extracted from DMRG (blue squares) compared to analytic results, eq.(8) (green dashed line), and including second order terms in t_2 (red full line). Other parameters are $\mu/U = 0.96 - 1.6t_1/U$, $\Delta\epsilon/U = 0.88 - 0.8t_1/U$ and $t_1/t_2 = 5$. (b) Density distribution at interface between topologically trivial $n = 1$ MI phase and topologically non-trivial $n = 1/2$ MI phase obtained by DMRG for $t_1/U = 0.5$, $t_1/t_2 = 5$ and $j_{\text{step}} = 16$. The inset shows the situation with t_1 and t_2 exchanged, corresponding to an interface between two topologically equivalent phases.

ify their topological nature we analyzed edge states between a topologically nontrivial MI with filling $n = 1/2$ and a MI with filling $n = 1$ using DMRG and analytic perturbative calculations. At the interface a stable and well localized edge state emerges, whose properties were studied in detail both analytically and numerically. Our numerical simulations verified that the many-body system supports exactly one localized, excited state within the bulk gap of the MIs. We argue that this is a result of the non-trivial topology of the $n = 1/2$ MI phase and notice that the edge state counting formula [16] carries over to the many-body winding number. In a grand-canonical setting the edge can have two different occupation numbers 0 or 1 in the interesting range of chemical potentials. The first case is characterized by a density dip at the edge of the $n = 1/2$ MI region below $1/2$. For finite values of U the second case results in a density peak at the edge of the $n = 1$ MI region with a local density exceeding 1 with a maximum value for intermediate values of t_1/U . These features allow a simple detection of the edge states and thus a verification of the different topological nature of the MI phases in cold-atom experiments. The required potential step can be realized by an admixture of a second heavy atom species in the presence of a weak harmonic confinement potential.

The authors thank E. Demler and J.Otterbach for stimulating discussions. F.G. thanks E. Demler and the physics department of Harvard University for hospitality during his visit and the graduate school MAINZ for financial support. Financial support from the DFG through SFB TR49 and from the reserach center OPTIMAS are gratefully acknowledged.

-
- [1] C.L. Kane and E.J. Mele, Phys. Rev. Lett. **95**, 146802 (2005).
 - [2] B.A. Bernevig, and S.C. Zhang, Phys. Rev. Lett. **96**, 106802 (2006); B.A. Bernevig, T.L. Hughes, S.-C. Zhang, Science **314**, 1757-1761 (2006).
 - [3] M.Z. Hasan, C.L. Kane, Rev. Mod. Phys. **82**, 3045-3067 (2010).
 - [4] Xiao-Liang Qi, Shou-Cheng Zhang Rev. Mod. Phys. **83**, 1057-1110 (2011).
 - [5] Von Klitzing, K.; Dorda, G. & Pepper, M. Phys. Rev. Lett. **45**, 494-497 (1980).
 - [6] Laughlin, R. B. Phys. Rev. B **23**, 5632-5633 (1981)
 - [7] D.J. Thouless, M. Kohmoto, M.P. Nightingale, and M. den Nijs, Phys. Rev. Lett. **49**, 405 (1982).
 - [8] G. Moore, and N. Read, Nuclear Physics B **360**, 362-396 (1991),
 - [9] I. Bloch, J. Dalibard, W. Zwerger, Rev. Mod. Phys. **80**, 885-964 (2008).
 - [10] E. Alba *et al.* Phys. Rev. Lett. **107**, 235301 (2011),
 - [11] L. Tarruel *et al.* Nature **483**, 302 (2012)
 - [12] N. Goldman, J. Beugnon, F. Gerbier, Phys. Rev. Lett. **108**, 255303 (2012)
 - [13] M. Atala, M. Aidelsburger, J.T. Barreiro, D. Abanin, T. Kitagawa, E. Demler, I. Bloch arXiv:1212.0572
 - [14] W.P. Su, J.R. Schrieffer, A.J. Heeger, Phys.Rev.Lett. **42**, 1698-1701 (1979)
 - [15] L.J. Lang, X.M. Cai, S. Chen, Phys. Rev. Lett. **108**, 220401 (2012)
 - [16] P. Delplace, D. Ullmo, G. Montambaux, Phys. Rev. B **84**, 195452 (2011).
 - [17] T. Gericke, P. Würtz, D. Reitz, T. Langen, H. Ott, Nature Phys. **4**, 949 (2008)
 - [18] W.S. Bakr, J.I. Gillen, A. Peng, S. Foelling, M. Greiner, Nature **462**, 74 (2009)
 - [19] J.F. Sherson, C. Weitenberg, M. Enders, M. Cheneau, I. Bloch, S. Kuhr, Nature **467**, 68 (2010)
 - [20] D. Muth, A. Mering, M. Fleischhauer, Phys. Rev. A **77**, 043618 (2008)
 - [21] P. Buonsante, V. Penna and A. Vezzani, Phys. Rev. A **70**, 061603(R) (2004).
 - [22] P. Buonsante and A. Vezzani, Phys. Rev. A **72**, 013614 (2005).
 - [23] J. Zak, Phys. Rev. Lett. **62**, 2747, (1989).
 - [24] S. Ryu, A. P. Schnyder, A. Furusaki, A. Ludwig, New J. Phys. **12**, 065010 (2010).
 - [25] S. R. White. Phys. Rev. Lett. **69**, 2863 (1992)
 - [26] U. Schollwöck, Ann. Phys. (New York) **326**, 96 (2011)
 - [27] F. Verstraete and J. I. Cirac, Phys. Rev. B **73**, 094423 (2006).
 - [28] J. K. Freericks and H. Monien Phys. Rev. B, **53**, 2691 (1996).
 - [29] P. Buonsante, V. Penna and A. Vezzani, Phys. Rev. B, **70**, 184520 (2004).
 - [30] Q. Niu, D. J. Thouless, Y. S. Wu, Phys. Rev. B **31**, 3372 (1985).
 - [31] M. V. Berry, Proc. Royal Soc. of London Series A-mathematical Physical and Engineering Sciences **392**, 45 (1984).
 - [32] A. Mering and M. Fleischhauer, Phys. Rev. A **77**, 023601 (2008).
 - [33] From its definition one can readily see that gauge transformations can change the Zak phase by multiples of 2π such that $\nu = \pm\pi$ are equivalent. The difference of signs is nevertheless well defined when infinitesimal sub-lattice breaking terms are included in the Hamiltonian (1).